Controlling DNA-Nanoparticle Serum Interactions

Supplementary Information

Kyryl Zagorovsky[1], Leo Y.T. Chou[1,2], and Warren C.W. Chan[1]*

[1]Institute of Biomaterials and Biomedical Engineering
Terrence Donnelly Centre for Cellular and Biomolecular Research
160 College Street, Room 450. Toronto, Ontario Canada. M5S 3E1
* Corresponding author. E-mail: warren.chan@utoronto.ca

[2]Present address:
Wyss Institute for Biologically Inspired Engineering, Harvard University
3 Blackfan Circle, Room 524/4A. Boston, Massachusetts USA. 02115
Dana-Farber Cancer Institute, Harvard Medical School
450 Brookline Avenue. Boston, Massachusetts USA. 02215

Table of Contents

Table S1. *List of DNA sequences used in the study*

Strand Name	Sequence
DNA25	***HS***–*AAAAAAAAAA*CCTATCGACCATGCT
DNA35	***HS***–*AAAAAAAAAA*CCTATCGACCATGCTCGAGCCTACA
DNA45	***HS***–*AAAAAAAAAA*CCTATCGACCATGCTCGAGCCTACAATCTCCAAGT
DNA55	***HS***–*AAAAAAAAAA*CCTATCGACCATGCTCGAGCCTACAATCTCCAAGTACTTACTCCG
cDNA25	AGCATGGTCGATAGG
cDNA35	TGTAGGCTCGAGCATGGTCGATAGG
cDNA45	ACTTGGAGATTGTAGGCTCGAGCATGGTCGATAGG
cDNA55	CGGAGTAAGTACTTGGAGATTGTAGGCTCGAGCATGGTCGATAGG
DNA45-*invT*	***HS***–*AAAAAAAAAA*CCTATCGACCATGCTCGAGCCTACAATCTCCAAGT(*invT*)
DNA45-*HP* *	***HS***–*AAAAAAAAAA*CCTATCGACCATGCTCGAGCCTACAATCTCCAA*GGGG*TTA*CCCC*G
DNA25-*invT*	***HS***–*AAAAAAAAAA*CCTATCGACCATGCT(*invT*)
DNA25-*5'* **	TAACAACGATCCCTC*AAAAAAAAAA*–***SH***
DNA45-*5'* ***	CCTATGGACCATGCTCGAGCCTACAATCTCCAAGT*AAAAAAAAAA*–***SH***
DNA25-*(diThiol)* ****	(***diThiol***)–*AAAAAAAAAA*CCTATCGACCATGCT
DNA45-*5'(diThiol)*	CCTATGGACCATGCTCGAGCCTACAATCTCCAAGT*AAAAAAAAAA*–(***diThiol***)
Assembled Structures	
Core-1	Same as DNA25
Core-1-*invT*	Same as DNA25-*invT*
Core-2	***HS***–*AAAAAAAAAA*CGAGTGAGTGCGACG
Sat-1	Same as DNA25-*3'SH*
Sat-1(***FAM***) *****	(*FAM*)**T**AACAACGATCCCTC*AAAAAAAAAA*–***SH***
Sat-2	GGTGGCTTACAGTCA*AAAAAAAAAA*–***SH***
Sat-3	***HS***–*AAAAAAAAAA*CACTGCCTGAACTGT
Sat-3(***Cy5***) *****	***HS***–*AAAAAAAAAA***T**(*Cy5*)CACTGCCTGAACTGT
Linker-1	GAGGGATCGTTGTTATACAGTTCAGGCAGTGTAGCATGGTCGATAGG
Linker-1-*invT*	GAGGGATCGTTGTTATACAGTTCAGGCAGTGTAGCATGGTCGATAGG(*invT*)
Linker-2	GCTCACTCACGCTGCCCACCGAATGTCAGT

* Underlined bases form the stem of the hairpin
** DNA25-5' is the same length as DNA25, but it's base sequence is different
*** Underlined base that was 'C' in the DNA45 sequence was replaced with 'G' to avoid strong hairpin formation
**** diThiol attachment achieved through a terminal dithiol phosphoramidite
***** The dye is conjugated to the underlined base

Discussion S1. *Aggregation of nanoparticles in serum*

When GNP-DNA constructs were added to serum they rapidly aggregated, forming large macromolecular clumps at the bottom of the tubes as early as 30 minutes into incubation (Suppl. Fig. S1). This resulted in the decrease in the 520 nm plasmon peak (characteristic of dispersed 15 nm gold nanoparticles (1)) and increased absorbance at longer wavelengths. The aggregation was reversible and could be dispersed by addition of protein degrading enzyme proteinase K (2) and sodium dodecyl sulfate (SDS). Addition of proteinase K alone resulted in almost complete recovery of non-aggregated absorbance profile, which indicated that the aggregation was largely mediated by serum proteins (Suppl. Fig. S1B). A similar serum-induced clustering of DNA functionalized nanoparticles was reported recently (3). To confirm whether small molecules played a role in aggregation we used 10kDa membrane to separate serum into its proteins and small molecular weight components (4). Aggregation was only observed in the case of complete serum (Suppl. Fig. S1C). This indicated that aggregation is caused by the combined interaction of proteins and small molecules with GNP-DNA surface and each other (Suppl. Fig. S1D, upper pathway).

Since DNA buried within a large nanoparticle cluster is inaccessible and therefore appears highly resistant to degradation, aggregation can introduce artefacts into the study of serum stability of GNP-DNAs. A common method to block protein adsorption onto nanoparticle is to saturate the surface with a thick layer of polyethylene glycol (PEG) (5-9). To check if passivation of nanoparticle surface with PEG could prevent aggregation, we backfilled the surface of GNP-DNA45 by PEG with molecular weights of 1, 2, 5, or 10 kDa at grafting density of 16000 PEG per nanoparticle (Suppl. Fig. S1D, lower pathway). Incubation of these nanoparticles in serum indicated that at least 5 kDa PEG was required

to prevent the formation of aggregates (Suppl. Fig. S1A,E). Shorter PEG molecules did not provide such protection, and backfilling with 1 kDa PEG actually enhanced the aggregation. The degree of aggregation could be quantified by collecting the clumped nanoparticles by mild centrifugation and washing them to remove non-aggregated nanoparticles. Aggregates were then re-suspended by proteinase K/SDS treatment and plasmon peak absorbance of re-dispersed nanoparticles measured (Supp. Fig. S1F). No plasmon absorption was observed for 5 and 10 kDa PEG even after 8 hours of incubation, confirming that none of the nanoparticles were present in the aggregated state in these samples. 1 kDa PEG backfill increased aggregation by around a factor of 2. This data suggests that if chosen incorrectly PEG can enhance rather than decrease serum-mediated aggregation.

Discussion S2. *Experimental measurement of relative length of DNA and PEG layer thickness*

Longer DNA is expected to require a corresponding longer PEG to maintain its steric protection against nuclease access. To further investigate this, we compared serum degradation of GNP-DNA45 backfilled with 5, 10, or 20 kDa PEG (Fig. 2C in the paper and Suppl. Fig. S4B). As the PEG size was increased from 5 to 10 kDa, degradation rate dropped from 0.55 hr^{-1} to around 0.1 hr^{-1}, which was the same as the rate observed for GNP-DNA25 and GNP-DNA35 backfilled with 5 kDa PEG (Fig. 2B). Switching to a larger 20 kDa PEG did not have any noticeable effect. We hypothesized that when the DNA strand is shorter than the thickness of the PEG layer, it is fully submersed within the PEG molecules and therefore strongly protected from protein binding. This is expected to be the case for DNA25 and DNA35 with 5 kDa PEG backfill and for DNA45 with 10 kDa and 20 kDa PEG. In contrast, the DNA that extends beyond the layer of PEG is exposed for degradation, which is predicted for DNA45 and DNA55 with the 5 kDa PEG layer. This hypothesis is also supported by the observation that whole lane densitometry of samples in Fig. 2 in the paper, which takes into account the total amount of DNA remaining on the nanoparticle instead of just the amount of full-length strand, DNA25 and DNA35 show similar degradation profiles, both of which are distinctly different from DNA45 and DNA55 (Suppl. Fig. S5A).

To determine the relative lengths of DNA strands and thicknesses of protective PEG layers, we first measured the hydrodynamic diameter (HD) of the gold nanoparticles grafted with PEG with and without DNA. Addition of DNA that was longer than the PEG layer thickness was expected to increase particle HD, while shorter DNA would have no effect. Contrary to expectations, DNA adsorption disrupted the formation of the PEG layer

and resulted in reduction in HD of the nanoparticles (Suppl. Fig. S5A). This made it impossible to directly determine the relative lengths of DNA and PEG, since observed HD decrease would mask any potential increase due to longer DNA. However, we noted that HD of DNA-only nanoparticles was larger in water, where strong repulsion between highly negatively charged DNA strands forced them into highly extended configuration, compared to PBS, where salt charge screening allowed for a more relaxed confirmation. If salts were removed (2X centrifugation at 16,000g, 35min each, using ultrapure water for resuspension) and then re-added to the original concentration (by addition of appropriate amount of 10X PBS), HD diameter remained unchanged, indicating the inter-strand repulsion was not strong enough to cause DNA desorption (Suppl. Fig. S5B). Since PEG is not a charged molecule (10), HD of PEG-only nanoparticles was not affected by addition of salts (Suppl. Fig. S5C). Therefore, an alternative method to compare DNA length and PEG layer thickness was to measure HD of these nanoparticles in water and PBS. The conformational changes of DNA strand that extend beyond the PEG layer would be expected to affect the HD of the nanoparticle (Suppl. Fig. S5D), while salt induced extension of a strand fully submerged within the PEG layer would not (Suppl. Fig. S5E). In agreement with the observations of DNA degradation, HD of DNA25 nanoparticles with 5 kDa PEG backfill and DNA45 with 10 kDa and 20 kDa PEG were not affected by addition of salts (Suppl. Fig. S5F), identifying DNA strand to be shorter than PEG layer thickness. HD was clearly affected by salts for DNA45 and DNA55 nanoparticles with 5 kDa PEG backfill, indicating extension of DNA strand beyond the protective layer of PEG. As a further confirmation, similar results were obtained when pH of the solution was lowered to 3 (Suppl. Fig. S5G). In acidic conditions protonation of the DNA backbone removes the

negative charge from DNA backbone, allowing the strands to settle into more compact configuration with decreased HD. In this case DNA35 was marginally affected by salt addition, suggesting comparable length of this DNA to the thickness of 5 kDa PEG backfill.

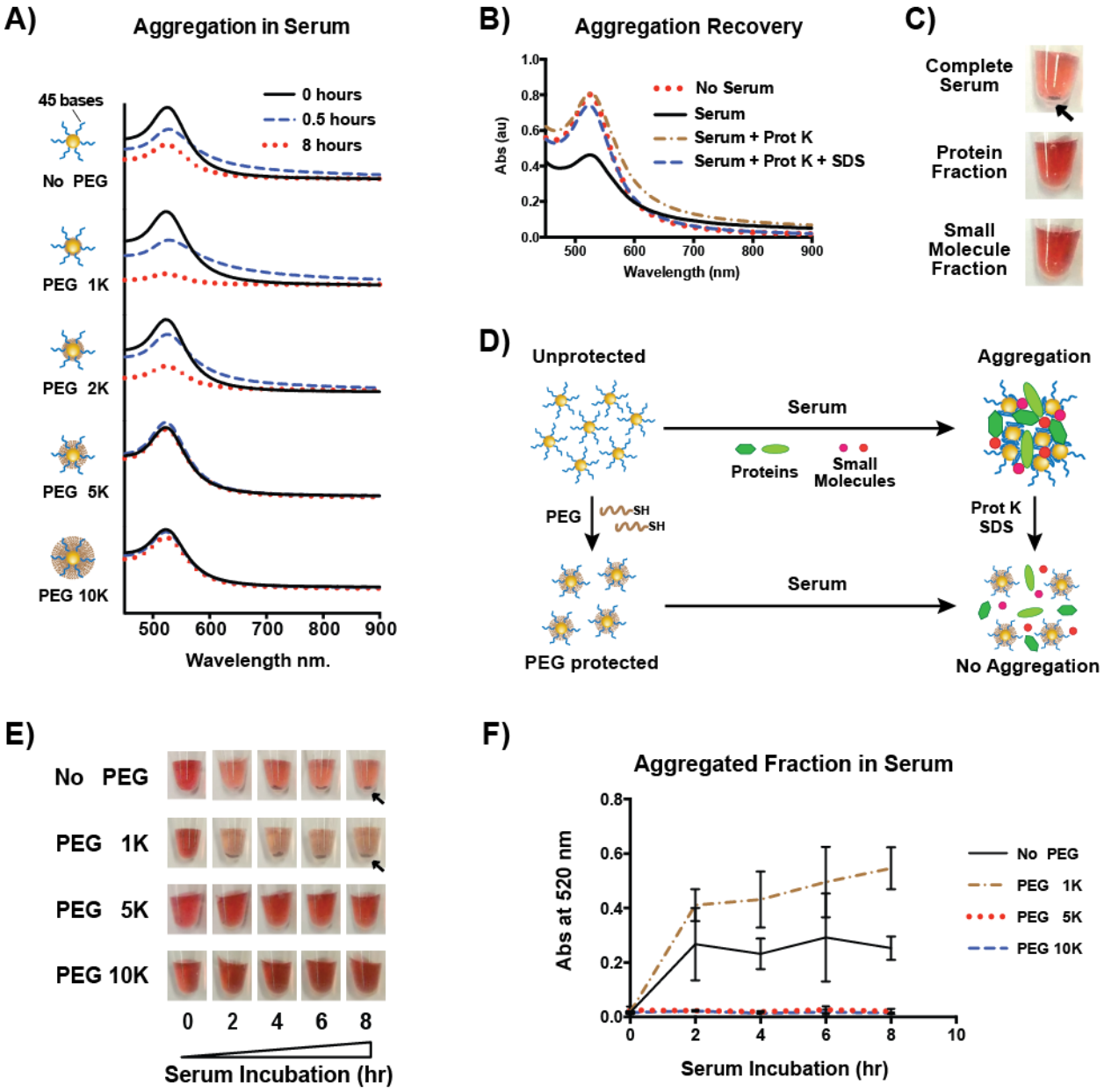

Figure S1. Aggregation of DNA-functionalized nanoparticles in serum. **A –** Absorbance spectra of nanoparticles incubated in serum at 37°C indicated rapid aggregation. Aggregation could be prevented by grafting protective layer of PEG of 5 kDa or larger. **B –** Aggregates could be re-dispersed by proteinase K and SDS treatment. **C –** Serum was separated into its protein and small molecule fractions by passing it through 10 kDa membrane. Aggregate formation (indicated by the arrow) only occurred in complete serum. **D –** Schematics of GNP-DNA aggregation in serum. Unprotected particles interact with proteins and small molecules to form large aggregate structures, which can be re-dispersed by proteinase K and SDS treatment. Protection by PEG backfill blocks this interaction and prevents aggregation. **E -** Visual tracking of serum aggregation of nanoparticles with different size PEG backfills. Aggregation occurs below PEG 5 kDa. The arrows indicate aggregate formation. **F –** Same as part E, but aggregation was tracked by purifying the aggregate by centrifugation, re-dispersing it with proteinase K and SDS, and measuring absorbance at 520 nm. Error bars are standard deviations based on 3 experimental replicates.

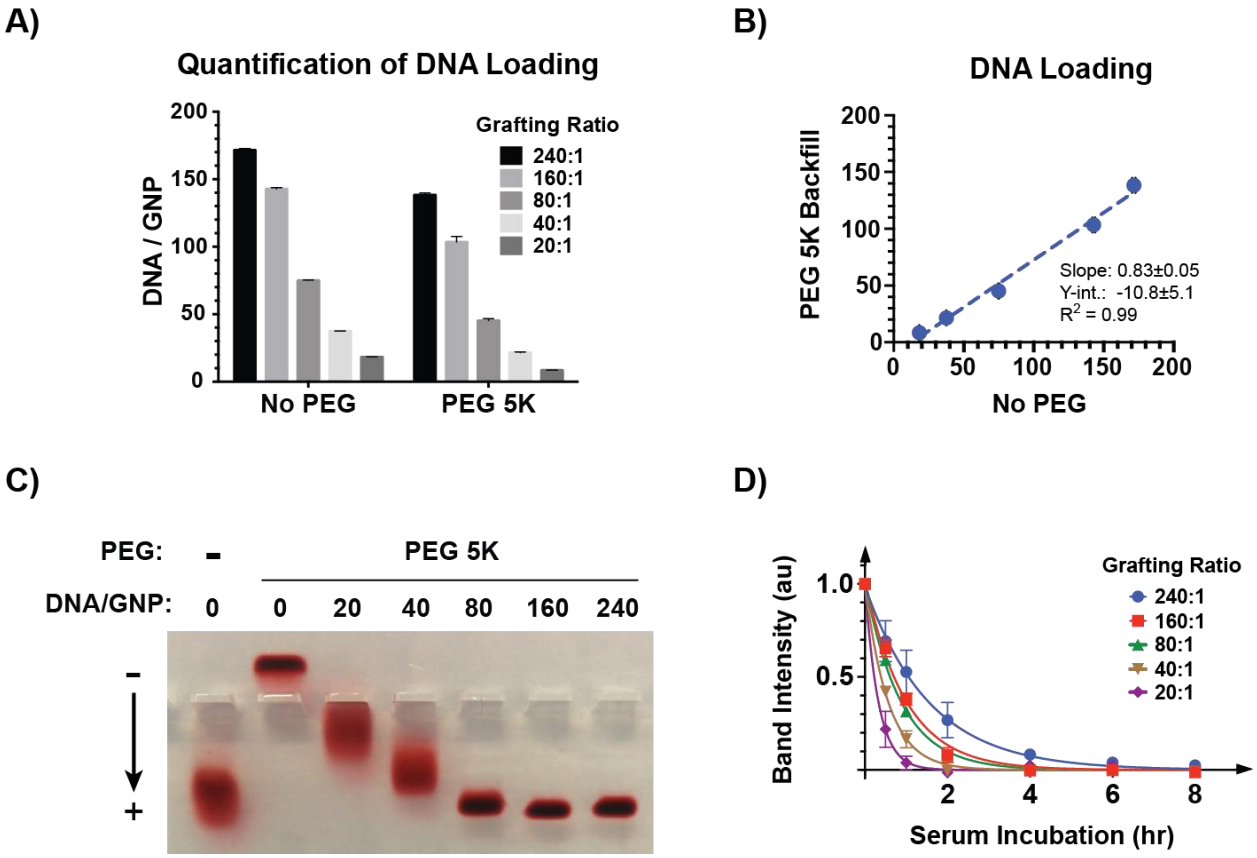

Figure S2. **A –** Quantification of DNA loading at different DNA to nanoparticle grafting ratios with and without 5 kDa PEG backfill. **B –** Linear fit performed for data from Part A to determine the DNA loading relationship for nanoparticles with and without PEG 5K backfill. Each data point represents particular DNA grafting ratio. **C –** Agarose gel electrophoresis of nanoparticles with 5 kDa PEG backfill and different DNA to nanoparticle grafting ratios. **D –** Band densitometry curves for Fig. 2A in the paper. Error bars are standard deviations based on 3 experimental replicates.

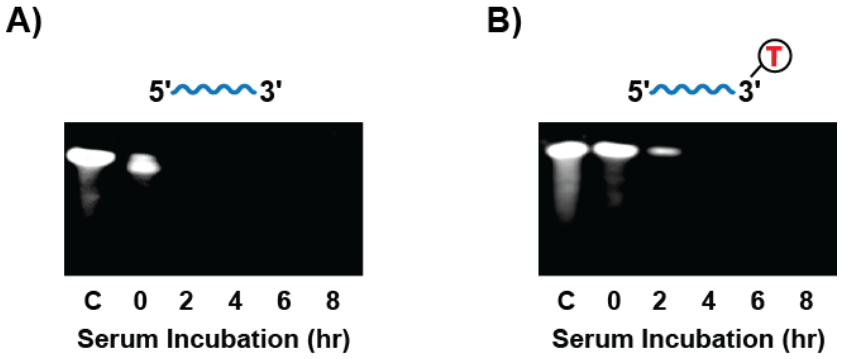

Figure S3. PAGE gel visualization of serum degradation of DNA strands free in solution. **A –** Degradation of 25 nt long DNA25. Much faster degradation is observed compared to the GNP-adsorbed DNA25 in Fig. 2B in the manuscript. **B –** Degradation of exonuclease inhibited DNA25-*invT*.

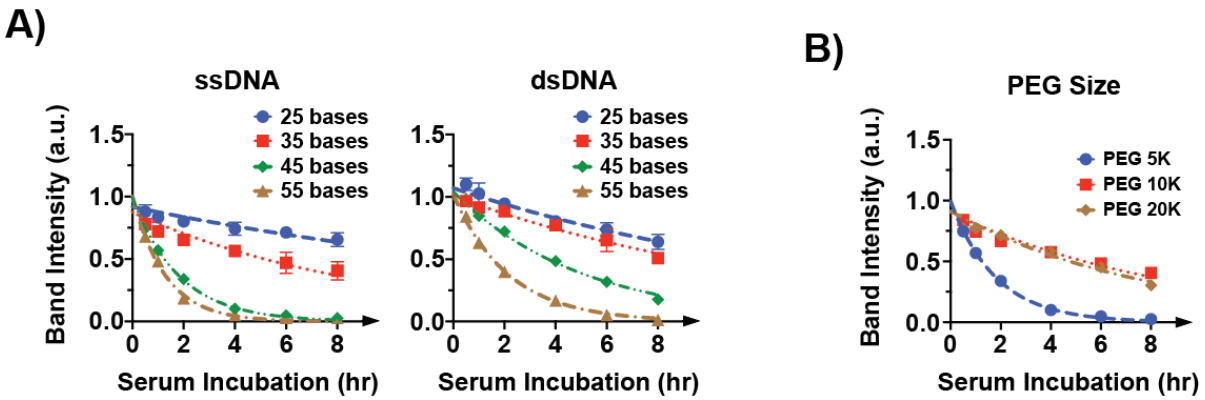

Figure S4. **A –** Band densitometry curves for Fig. 2B in the paper. **B –** Band densitometry curves for Fig. 2C in the paper. Error bars are standard deviations based on 3 experimental replicates.

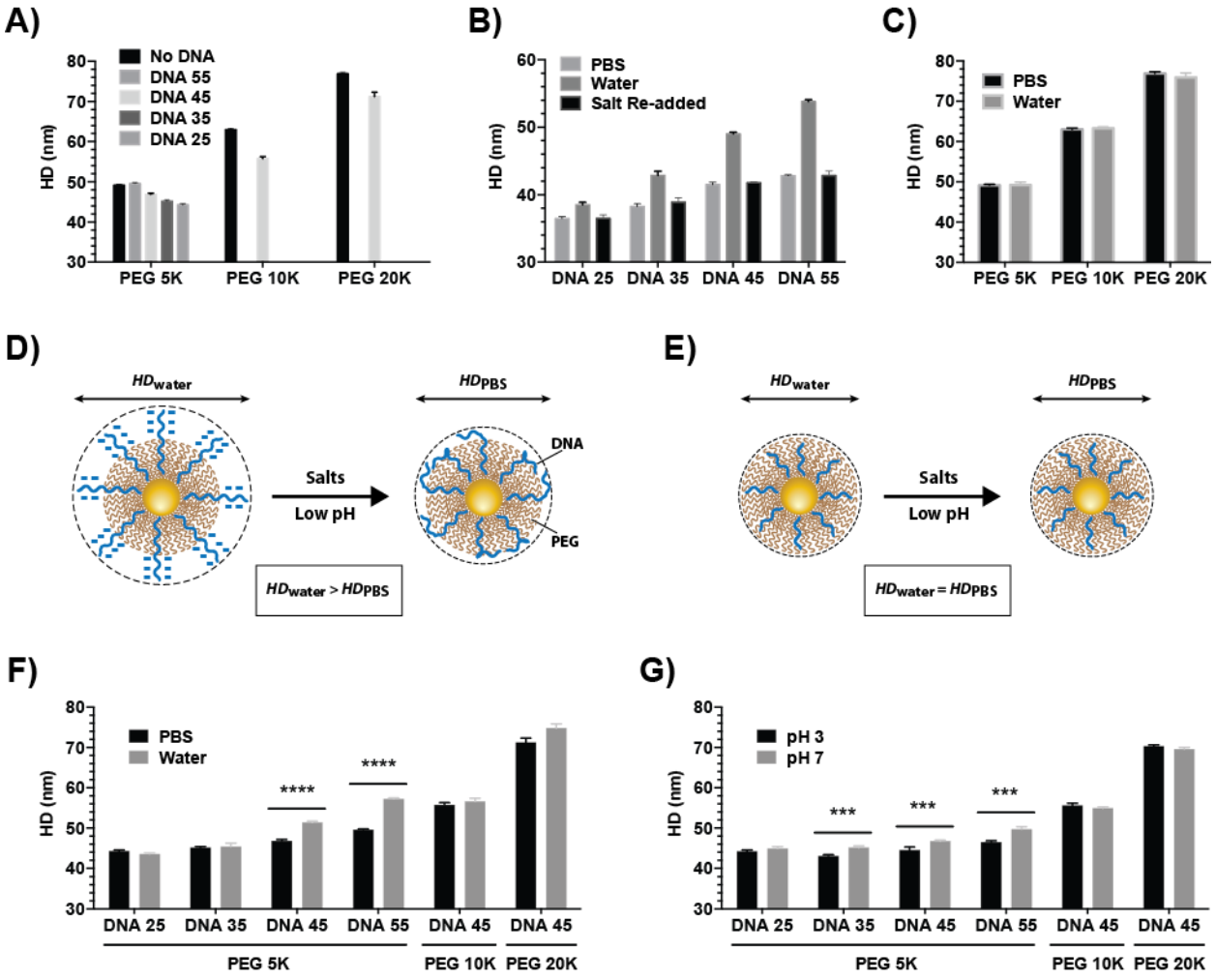

Figure S5. Investigation of relative length of DNA strands and thickness of protective PEG layer. **A –** Hydrodynamic diameter (HD) of nanoparticles as a function of DNA length and PEG size. Only DNA45 was used with 5 kDa and 10 kDa PEG. **B –** Effect of salts on HD of nanoparticles with different lengths of DNA but no PEG backfill. HD was first measured in PBS, then nanoparticles were centrifuged and HD measured after resuspension in water. 10X PBS was then used to bring salt concentration back to 1X PBS levels, and HD measured again. **C –** Effect of salts on HD of nanoparticles grafted with PEG, but not DNA. **D** and **E –** Schematic representation of the effect of salts on HD of nanoparticles functionalized with DNA and backfilled with PEG. When DNA that extends beyond the thickness of the PEG layer (**D**) is placed in water, strong repulsion between highly negatively charged DNA strands forces them to maximally extend away from the particle. When salts are added, they screen the negative charge allowing the DNA to fold onto the nanoparticle, which reduces HD. In contrast, when DNA strand is shorter than PEG layer (**E**), HD is determined by the size of the PEG layer rather than DNA extension, and therefore is not affected by the presence of salts. Lowering solution pH is expected to yield similar results, since DNA is protonated in acidic conditions, removing its negative charge. **F –** Comparison of HD of the nanoparticles with different DNA length and PEG sizes in PBS and water. **G –** Comparison of HD of the nanoparticles with different DNA length and PEG sizes in solution with pH 3 and pH 7. Error bars are standard deviations of the HD mean based on three measurements. Statistical significance was determined by and unpaired t-test.

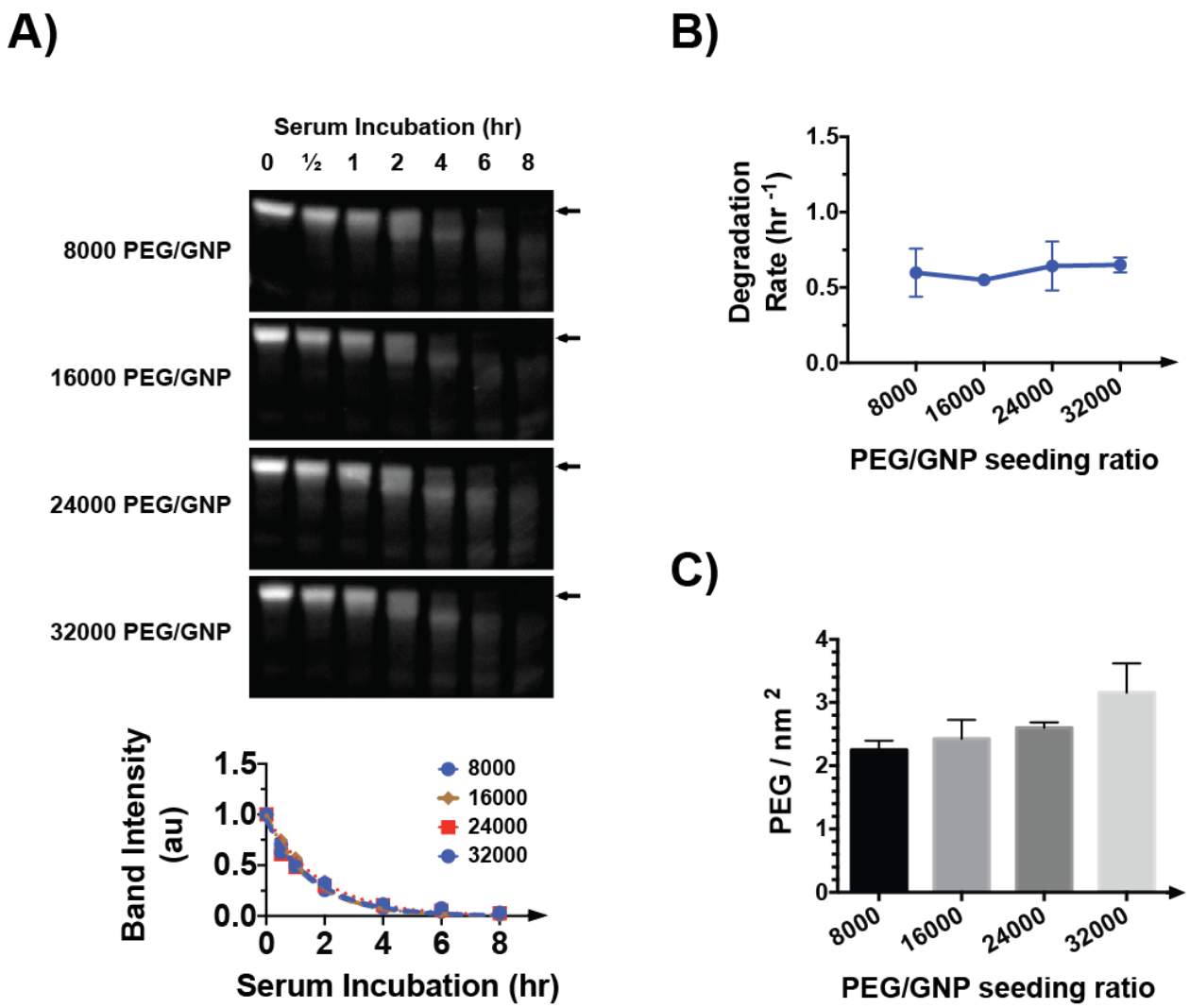

Figure S6. A – PAGE gel data and band densitometry curves for serum degradation of nanoparticles with DNA45 and 5 kDa PEG grafted at different PEG-to-nanoparticle ratios. **B –** Degradation rates calculated from the densitometry curves in Part A. No statistical significance was observed between the different grafting ratios based on an unpaired t-test. **C –** Quantification of PEG surface density as a function of grafting ratio. For parts A and C error bars are standard deviations; for part B error bars represent 95% confidence interval associated with the degradation rate curve fitting; all data based on three experimental replicates, representative PAGE gel data is shown.

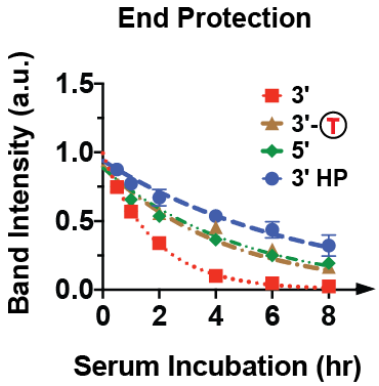

Figure S7. Band densitometry curves for Fig. 3A in the paper. Error bars are standard deviations based on 3 experimental replicates.

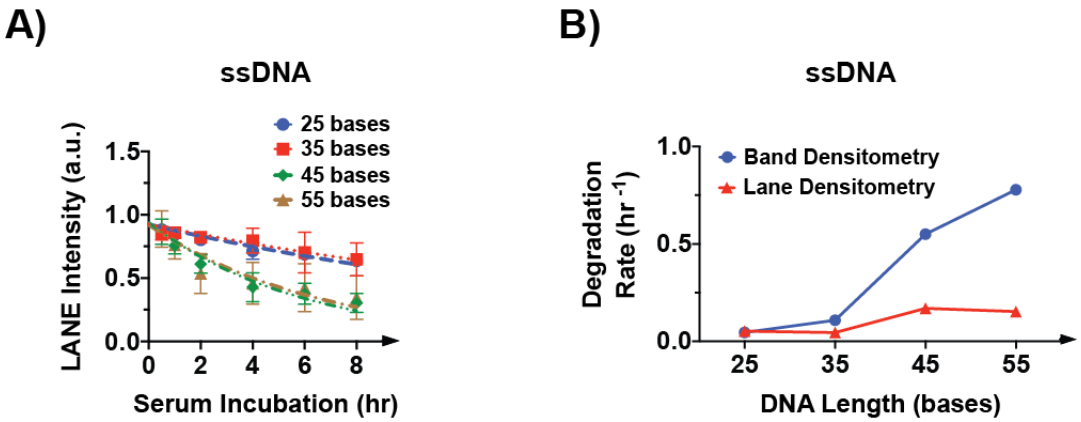

Figure S8. **A –** PAGE gel lane densitometry for serum incubation of nanoparticles with single-stranded DNA25, DNA35, DNA45 and DNA55 (gel images are presented in Fig. 2B in the paper). **B –** Degradation rates calculated based on lane densitometry are compared to those determined from band densitometry (Fig. 2B). Band densitometry only considers the signal from the band associated with the full-length DNA strand. In contrast, lane densitometry includes the total signal coming from the whole gel lane, which contains both the bands associates with the full size strand and all of its shorter degradation products (e.g., the smear plus any discreet bands). As exonucleases or endonucleases degrade the DNA, they produce shortened degradation products, while desorption removes the whole strand. From band densitometry perspective the two processes are similar, since reduction in the signal from the band associated with full-length oligonucleotide is the same whether the strand is shortened or removed. However, from lane densitometry perspective any cleaved or partially degraded DNA strand still retains a portion of its signal when visualized on the gel. In contrast, a desorbed strand looses 100% of its signal. Therefore, the lane signal decreases slower than full-size band signal in the case of strand degradation, while for desorption the rate of change associated with the two measurements is the same. Error bars are standard deviations based on 3 experimental replicates.

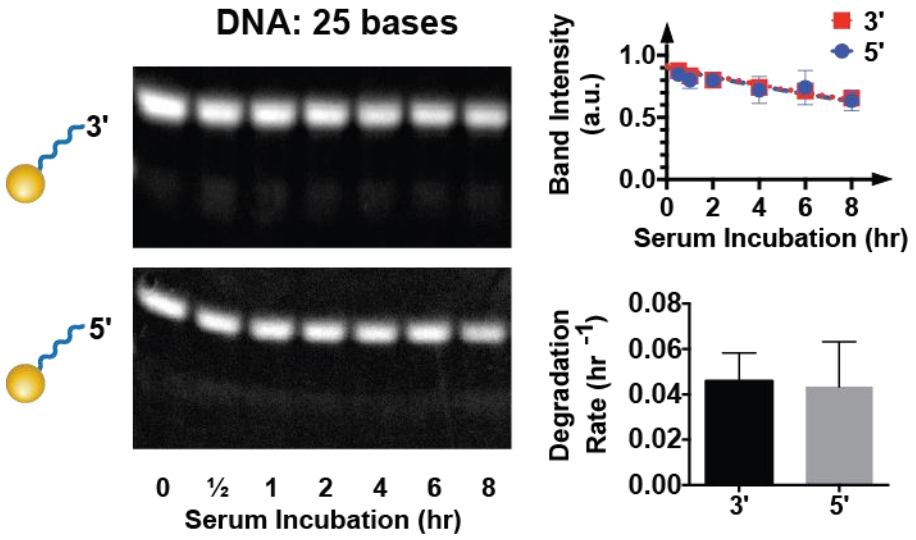

Figure S9. Comparison of serum degradation of 25 bases long DNA with 3' or 5' terminal ends. Error bars for densitometry curves are standard deviations based on three experimental replicates. The rates are obtained from the single-phase decay fits of the densitometry curves, error bars are 95% confidence intervals associated with the fit. No statistically significant difference was observed based on an unpaired t-test. Representative PAGE gel data is shown.

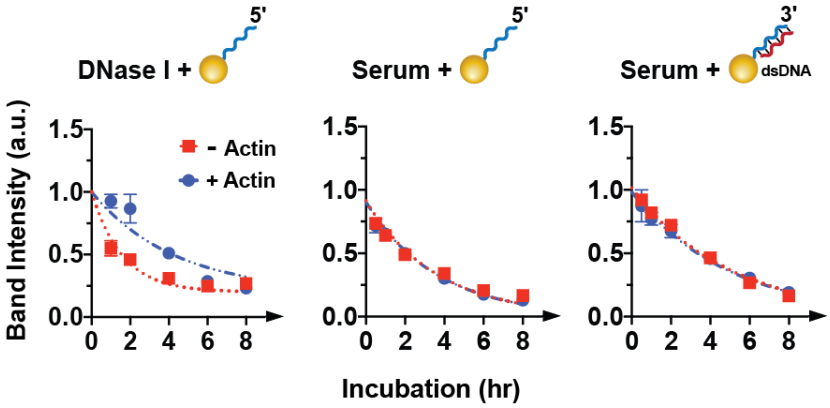

Figure S10. Band densitometry curves for Fig. 3B in the paper. Error bars are standard deviations based on 3 experimental replicates.

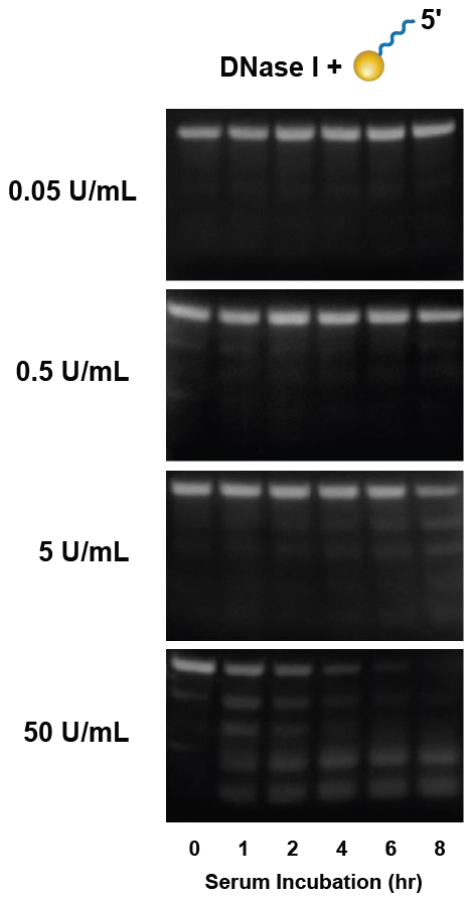

Figure S11. Determining DNase I concentration required to observe detectable DNA45-5' degradation on gold nanoparticle surface.

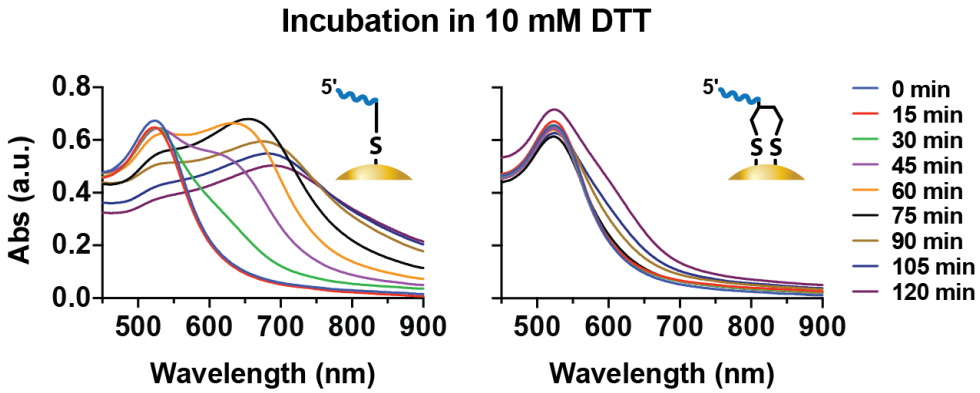

Figure S12. DNA adsorbed through di-thiol linker makes gold nanoparticles resistant to DTT treatment. Nanoparticles with DNA45 adsorbed through mono-thiol or di-thiol linkers were incubated for 120 minutes at 37°C in 10 mM DTT. Aggregation was indicated by the shift of the 520 nm plasmon absorbance peak to longer wavelengths.

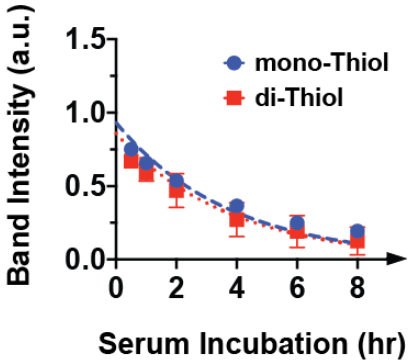

Figure S13. Band densitometry curves for Fig. 3C in the paper. Error bars are standard deviations based on 3 experimental replicates.

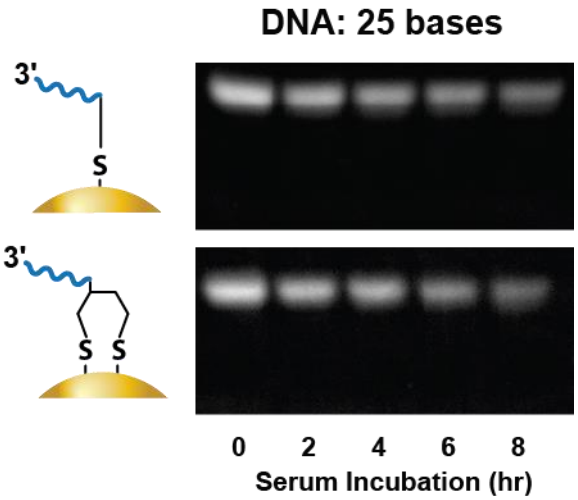

Figure S14. Comparison of degradation of DNA25 adsorbed onto nanoparticle surface through mono-thiol or di-thiol linker.

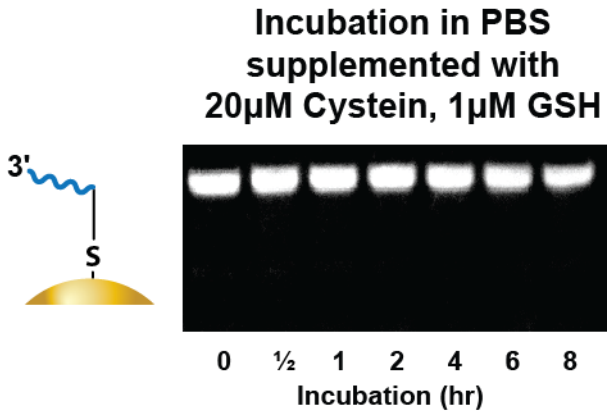

Figure S15. Serum concentrations of free thiol-containing small molecules are not sufficient to eject DNA strands from gold nanoparticle surface. Nanoparticles with DNA45-*5'* adsorbed through mono-thiol linker were incubated in PBS supplemented with 20 μM Cysteine (mimics combined contribution of cysteine and homo-cysteine, each present in serum at ~10 μM (11)) and 1 μM GSH at 37°C for 8 hours.

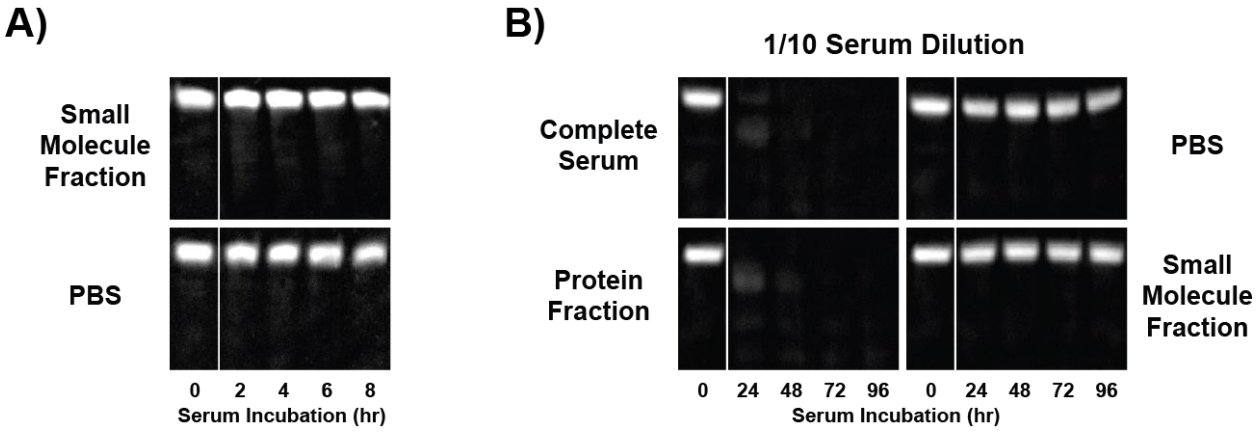

Figure S16. **A –** Incubation of nanoparticles with DNA45 and 5 kDa PEG backfill in small molecule fraction of undiluted serum is identical to PBS treatment, indicating that small molecules are not involved in DNA degradation. **B –** Incubation of nanoparticles with 3' exonuclease resistant DNA45-*5'* and 5 kDa PEG backfill in 10 times diluted serum and its protein or small molecule fractions at 37°C for 96 hours. One concern when using 10 kDa membrane was that concentrated serum was a highly dense liquid which could clog the membrane and trap small molecules, leading to reduced concentration of small molecules in the filtrate. To address this we diluted serum 10 times before filtration and no clogging was observed. Diluted serum fractions were then incubated with DNA45-5' nanoparticles to specifically look at desorption rather than enzymatic degradation. To account for serum dilution incubation was performed for up to 96 hours. Protein fraction yielded similar results to complete serum and no desorption was observed for the small molecule fraction or in PBS, confirming that desorption process is carried out by proteins.

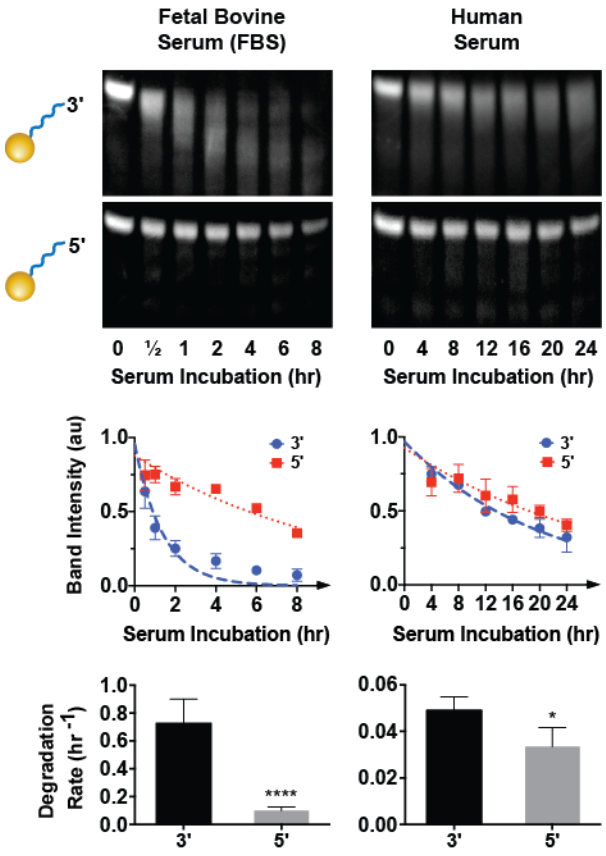

Figure S17. Incubation of nanoparticles with DNA45 or DNA45-5' and 5 kDa PEG backfill in fetal bovine serum (FBS) or human serum. Error bars for the densitometry curves are standard deviations. Fits for the degradation rates are based on three experimental replicates, error bars are 95% confidence intervals associated with the fit. Representative PAGE gel data is shown. Statistical significance was determined by an unpaired t-test.

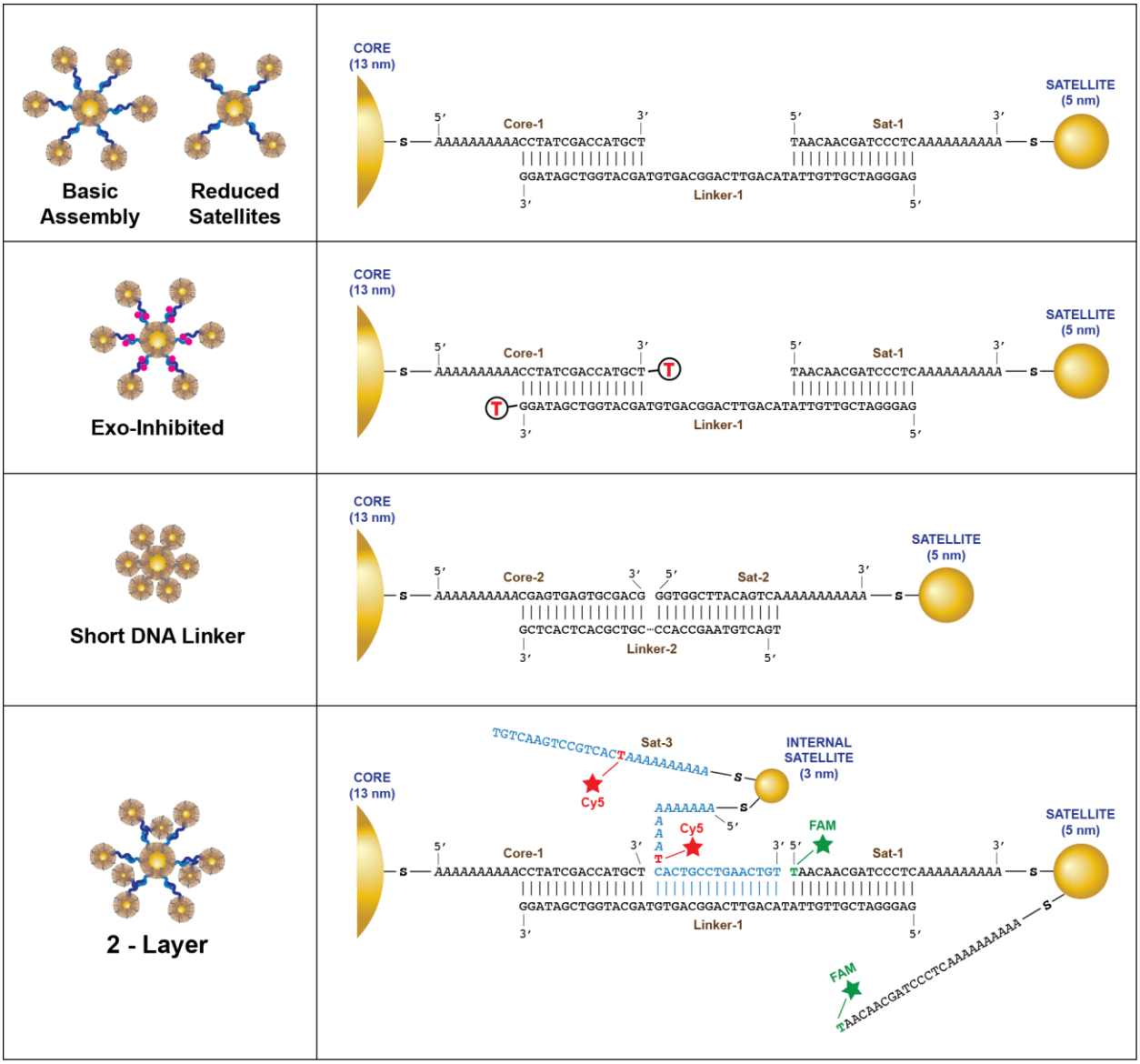

Figure S18. Molecular details of the five core-satellite structures used in the study. 'Basic Assembly' and 'Reduced Satellites' contained identical DNA sequences, but differed in ratio of satellites to the core. 'Exo-inhibited' structures were protected from DNase I degradation by blocking all free 3' ends with inverted T base. In the case of 2-Layer structure DNA was only labeled with the fluorescent dye (at bases indicated in the figure) for the experiments described in Fig. 5 in the paper. Strands adsorbed onto 2-Layer structures used for experiments shown in Fig. 5 were not labeled. Sat-1, Sat-2 and Sat-3 strands were isotropically distributed around the satellite nanoparticles, and only 1 or 2 of these were expected to participate in the core-satellite linkage, the rest would remain non-hybridized (demonstrated in the case of the 2-Layer structure). Therefore, FAM dyes conjugated to Sat-1 strands would be spherically spread out around the outer satellite layer, and Cy5 dyes would surround the inner layer. All single-layer structures were synthesized with 5 kDa PEG backfill. 2-Layer structures were synthesized either with 5 kDa PEG (structure used in Fig. 4 and Fig. 5) or 10 kDa PEG backfill (structure used in Suppl. Fig. S21)

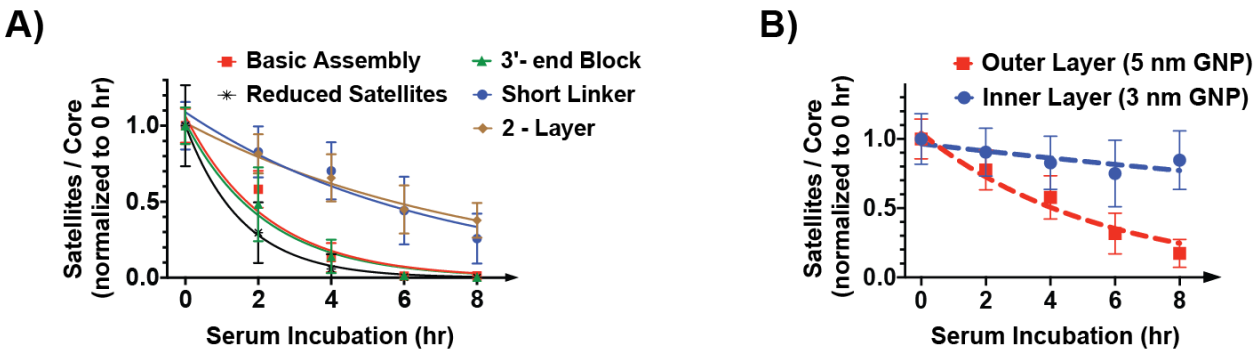

Figure S19. Quantification of serum breakdown of assembled structures for the experiment described in Fig. 4 in the paper. **A –** Number of satellites per core nanoparticle remaining after indicated serum incubation time were quantified by TEM. Data fitted with the single-phase decay curves. **B –** For 2-Layer structures the number of outer layer 5 nm diameter satellites were quantified separately from the inner layer 3 nm satellites. TEM images and associated degradation rates are presented in Fig. 4. The results were averaged over 50 or more assemblies, normalized to core-to-satellite ratios of the intact structures at time 0 hr and fitted with single-phase decay curves. Error bars are standard deviations.

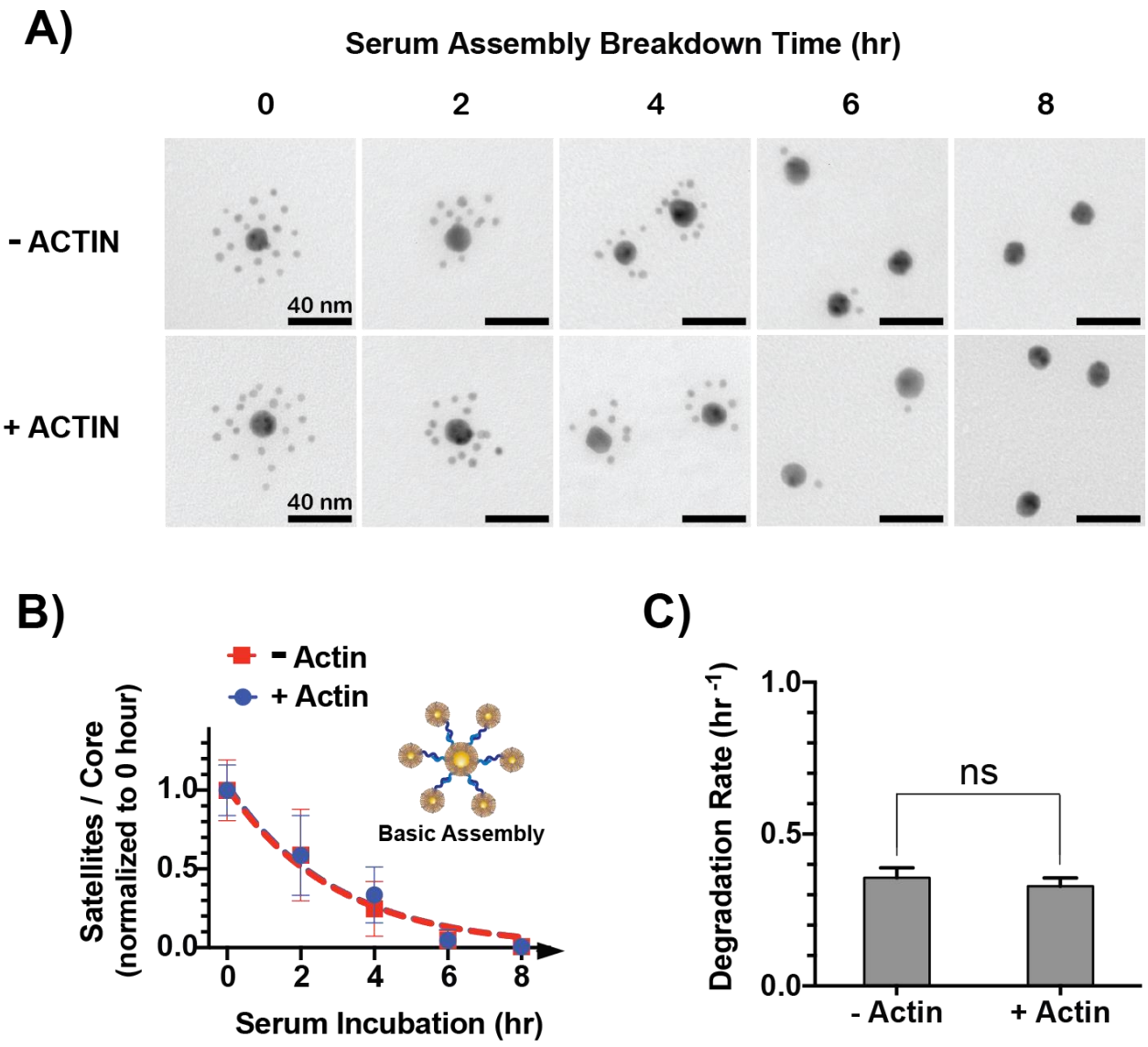

Figure S20. Serum degradation of Basic Assembly structures with and without actin as DNase I inhibitor. **A –** representative TEM data of structure breakdown. **B –** Number of satellites per core nanoparticle remaining after indicated serum incubation time, averaged over 50 particles. Satellite-to-core ratio was quantified by direct counting of nanoparticles in TEM images, normalized to the ratio of intact structures at 0 hr. Error bars are standard deviations. **C –** The data from Part B was fitted with a single-phase decay curve to obtain degradation rates. Error bars represent 95% confidence intervals associated with the fits. Statistical significance was determined by an unpaired t-test. Actin treatment does not show any significant effect on degradation.

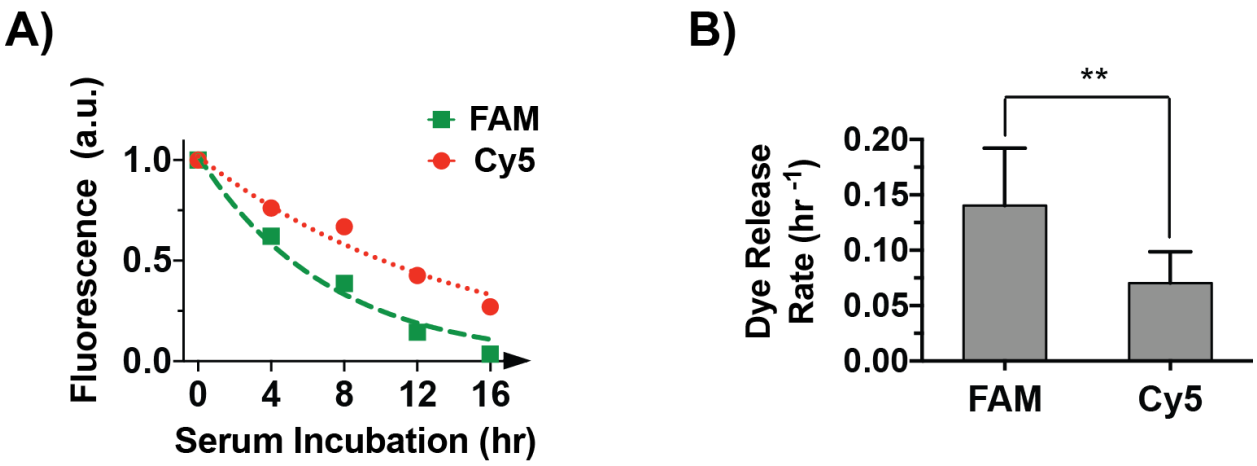

Figure S21. FAM and Cy5 serum release from 2-Layer assemblies identical to those presented in Fig. 5 in the paper, but backfilled with larger 10 kDa PEG. The release profiles are similar to those of 5 kDa PEG structures (**A**), but the respective degradation rates are slower for both dyes (**B**). Therefore, the size of protective PEG layer can be used to tune cargo release rates. Error bars represent 95% confidence interval associated with the one-phase decay fit of the degradation rate. Statistical significance determined by an unpaired t-test.

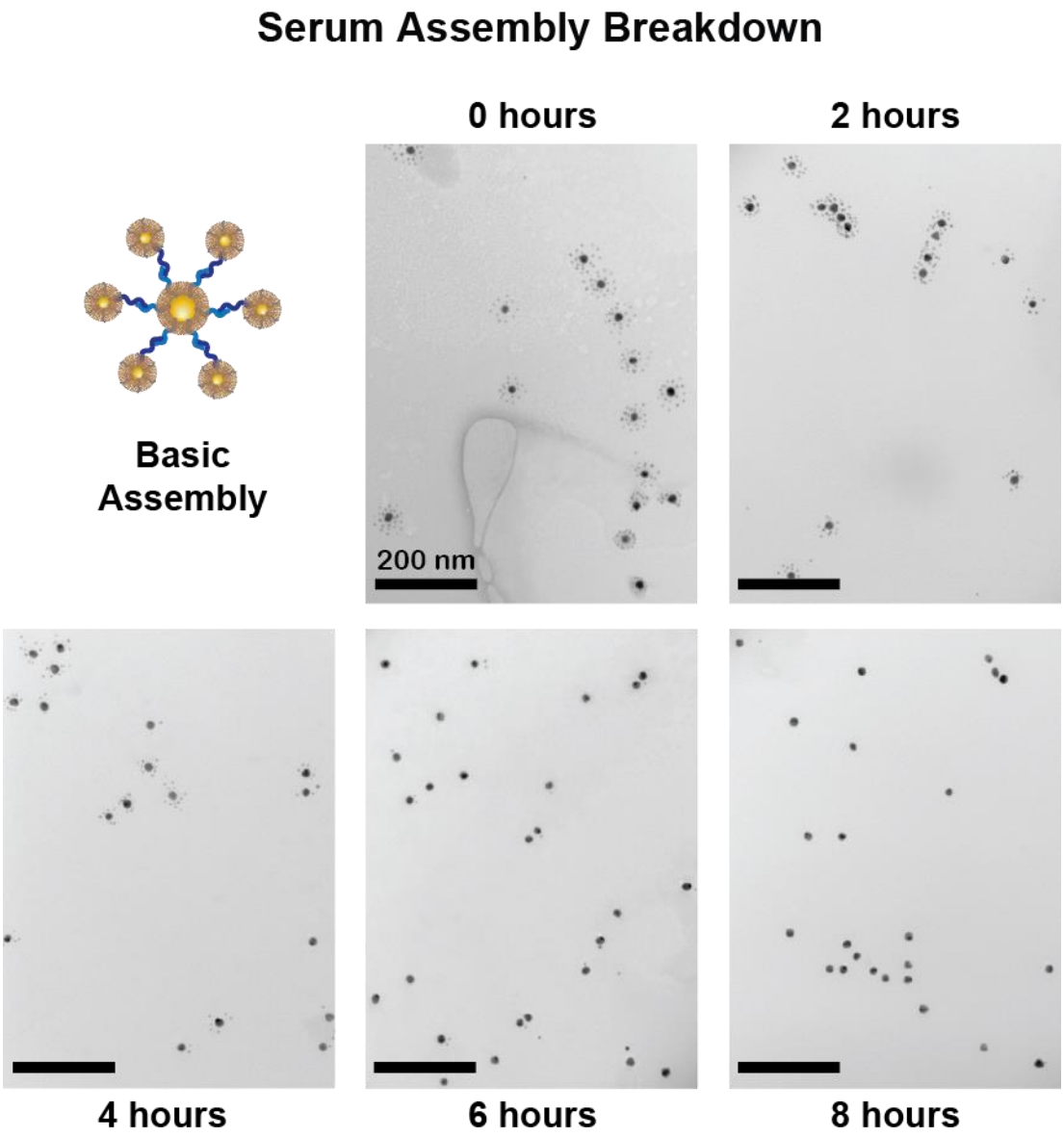

Figure S22. Lower magnification images for serum degradation of 'Basic Assembly' in Fig. 4 in the paper.

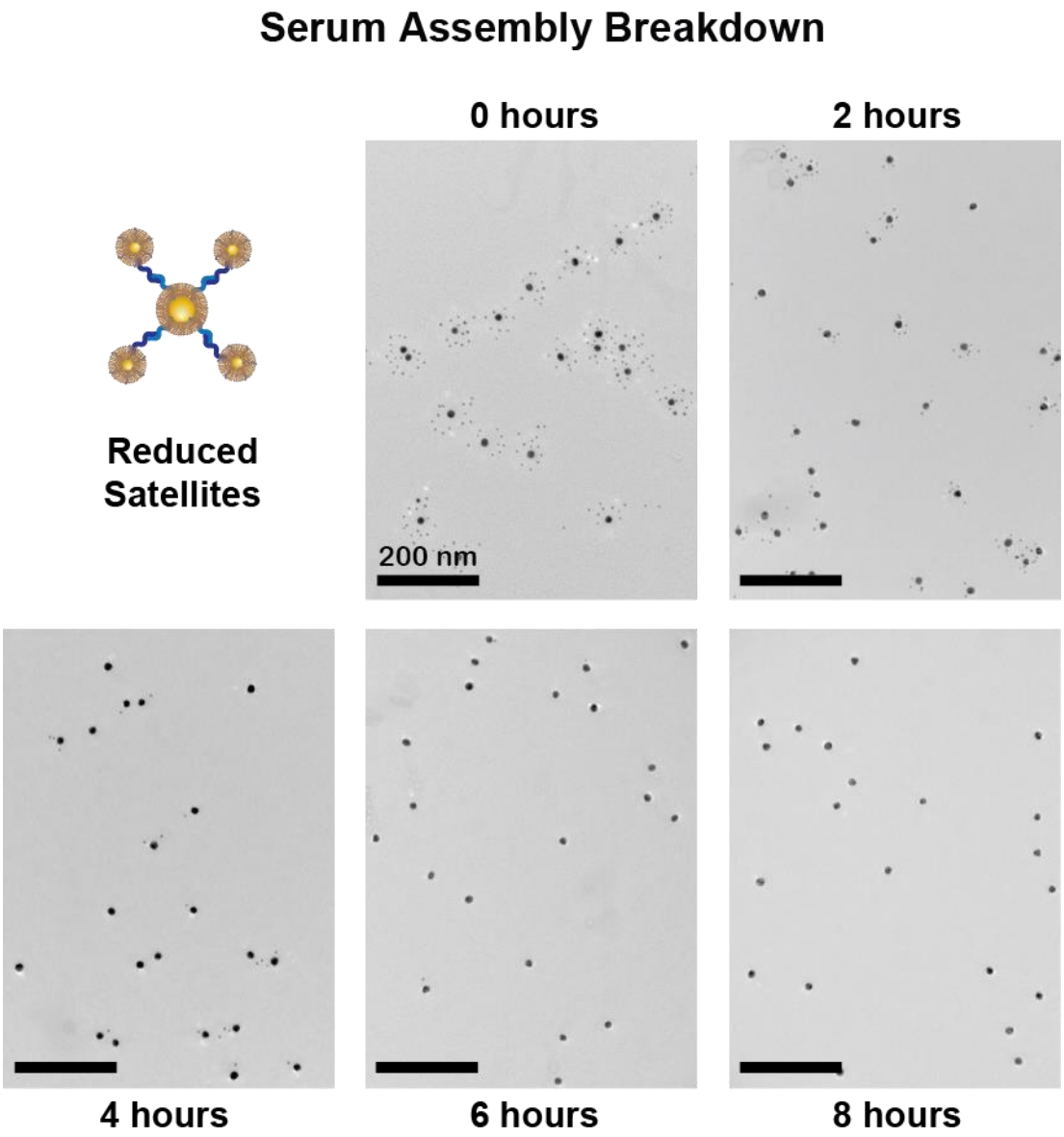

Figure S23. Lower magnification images for serum degradation of 'Reduced Satellites' in Fig. 4 in the paper.

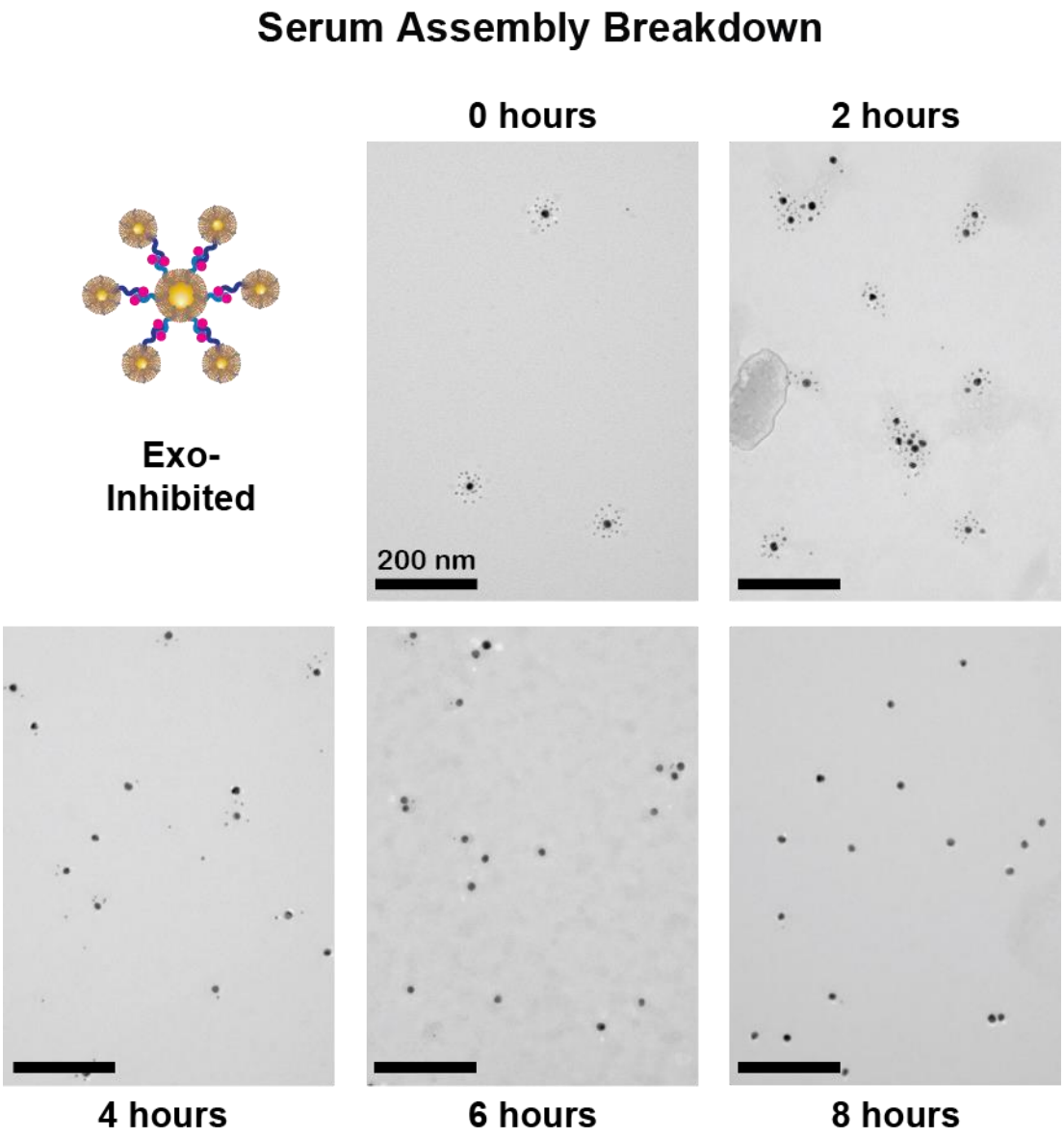

Figure S24. Lower magnification images for serum degradation of 'Exo-Inhibited' in Fig. 4 in the paper.

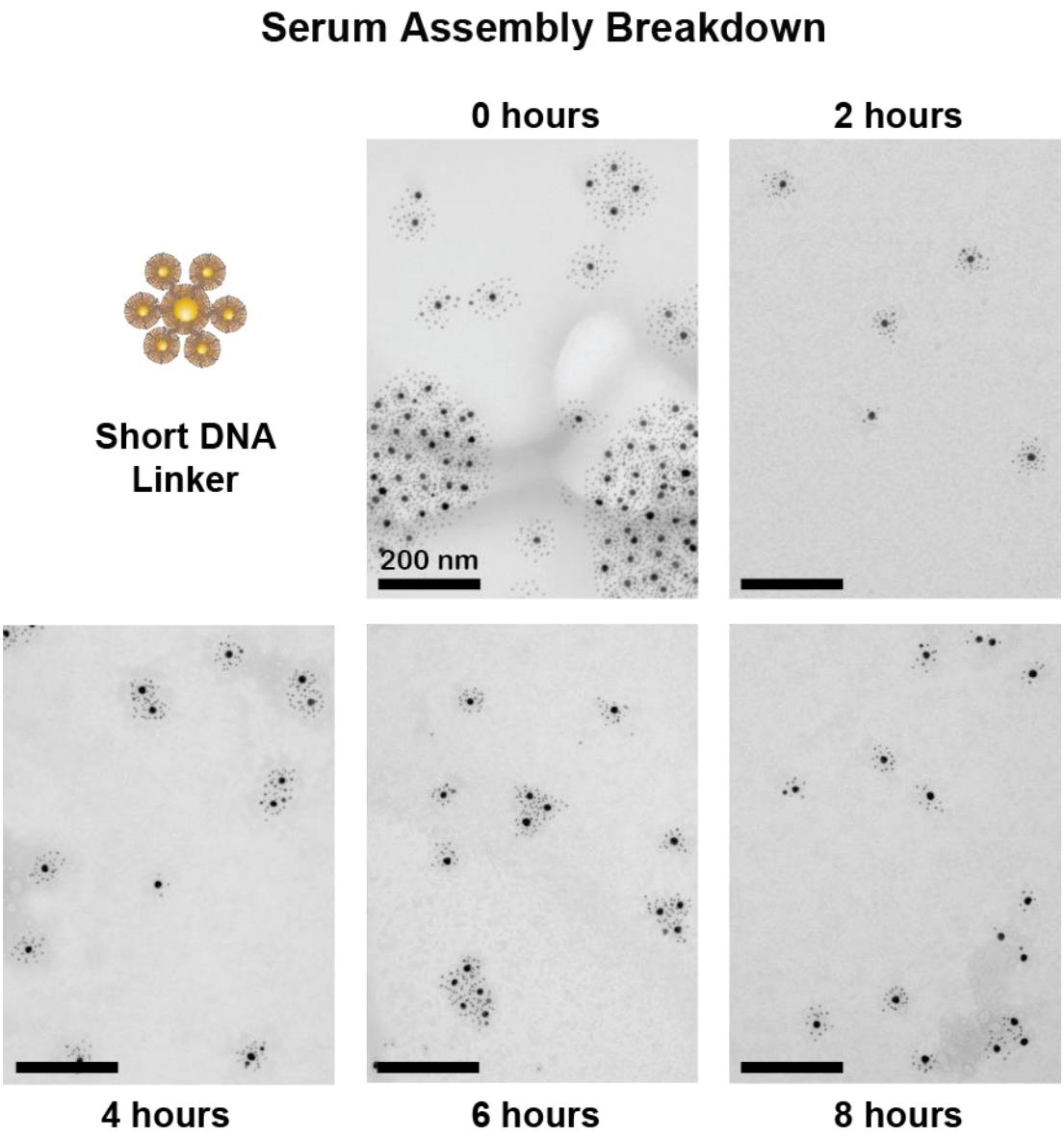

Figure S25. Lower magnification images for serum degradation of 'Short DNA Linker' in Fig. 4 in the paper.

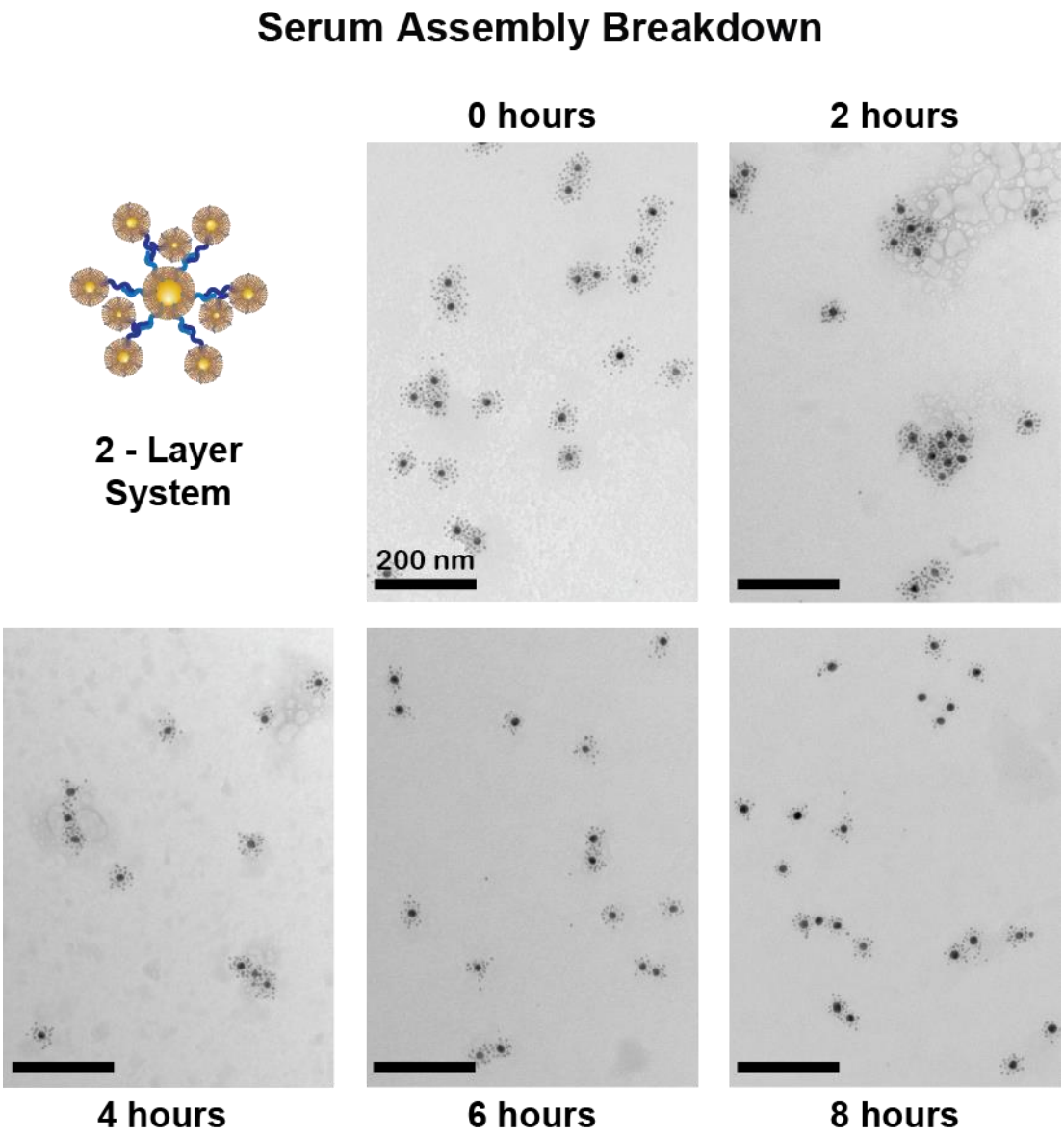

Figure S26. Lower magnification images for serum degradation of '2-Layer System' in Fig. 5 in the paper.

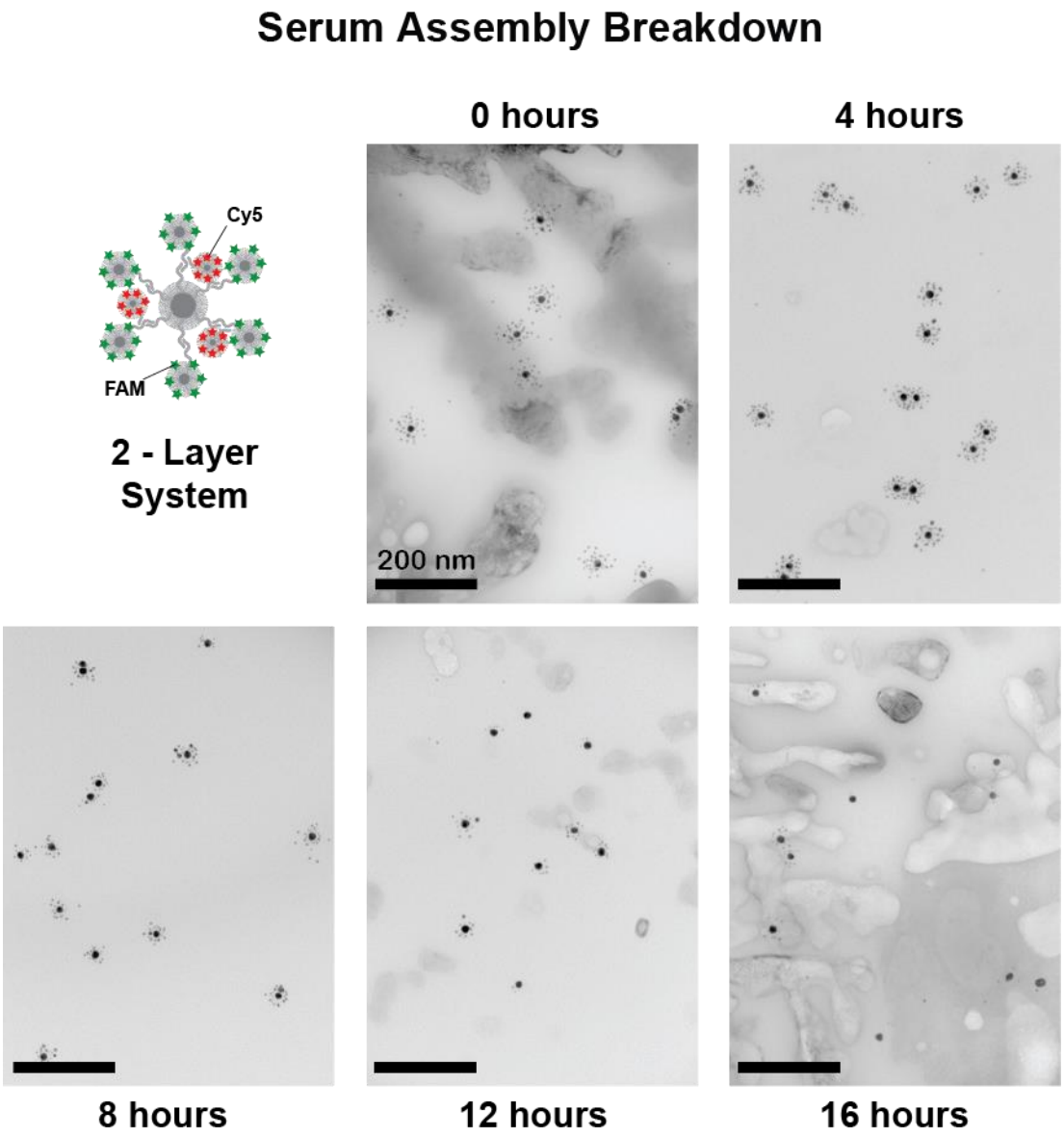

Figure S27. Lower magnification images for serum degradation of '2-Layer System' in Fig. 6 in the paper.

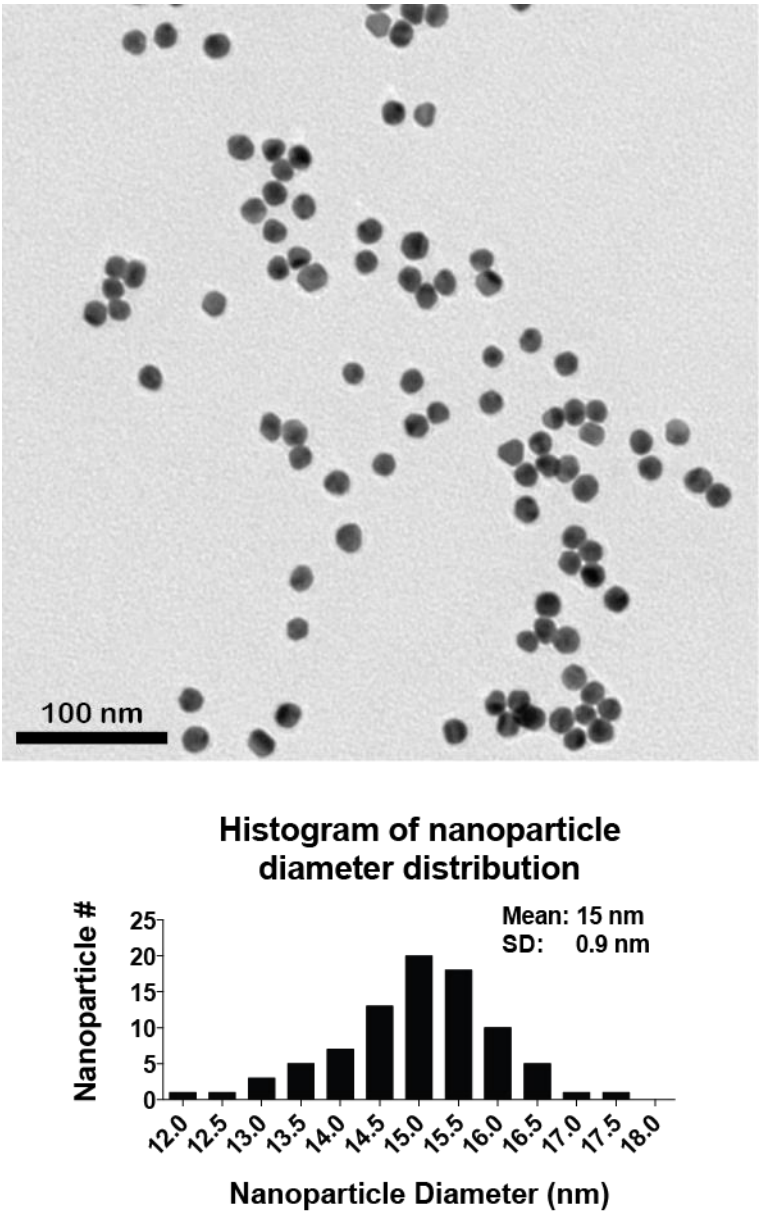

Figure S28. TEM and size distribution of 15nm GNPs.

MATERIALS AND METHODS

Chemicals and Materials. General chemicals were purchased from Sigma-Aldrich, BioShop (Burlington, ON), and Caledon Laboratories (Georgetown, ON). Polyethylene glycol was purchased from Laysan BIO (Arab, AL) and NOF Corporation (Tokyo, Japan). PAGE gels were purchased from Invitrogen. All DNA was purchased from Bio Basics (Markham, ON) as lyophilized pellets purified by HPLC or PAGE. See SI for more detailed information.

$HAuCl_4$, sodium citrate tribasic, sodium phosphate monobasic, sodium phosphate dibasic, sodium dodecyl sulphate, magnesium chloride, potassium chloride, *tris*(2-carboxyethyl)phosphine (TCEP), glutathione (GSH), cysteine and Ellman's reagent were purchased from Sigma-Aldrich. Sodium chloride, Tween-20, Tris, proteinase K, and dithiothreitol (DTT) were purchased from BioShop (Burlington, ON, Canada). Hydrochloric acid and nitric acid were purchased from Caledon Laboratories (Georgetown, ON, Canada). Thiolated methoxyl polyethylene glycol MW=1 kDa was purchased from Laysan BIO (Arab, AL). Quant-iT OliGreen ssDNA assay kit and PAGE gels were acquired from Invitrogen. mPEG-SH with molecular weights of 2, 5, 10 and 20 kDa were purchased from NOF Corporation (Tokyo, Japan). Serum was purchased from Sigma-Aldrich (M5905-500ML). All DNA sequences were purchased from Bio Basic (Markham, ON, Canada) purified (thiol-functionalized sequences were purified by HPLC and non-functionalized ones by PAGE purification) and lyophilized by the company. All lyophilized DNA sequences were re-suspended in ultrapure distilled water to 100 μM concentration and stored at -20°C. DNA sequences used in the study are outlined in Table S1**.**

Nanoparticle Synthesis. Gold nanoparticles (GNPs) were synthesized by citrate reduction methods described previously. To make 15nm GNPs, 1mL of 1% (w/v) $HAuCl_4$ solution was added to 98 mL of ultrapure water in 250 mL Erlenmeyer flask and the mixture brought to rapid boil on stir plate set to 300°C. 1mL of 3% (w/v) trisodium citrate was then quickly injected under intense stirring and mixture kept on heated stir plate for 10 min, then cooled on ice. TEM images with calculated size distribution are shown in Suppl. Fig. S28.

To make 3nm and 5nm gold nanoparticles 1mL of 1% (w/v) HAuCl4 was added to 80mL of ultrapure water in a 250 mL Erlenmeyer flask and heated on stir plate set to 60°C. In parallel, a reducing solution was prepared by mixing the reagents in the amounts listed in the table:

Nanoparticle size (nm)	**3**	**5**
Water (mL)	12.7	16.0
1% Trisodium citrate	4.0	4.0
1% Tannic acid	2.7	1.0
3.46mg/mL Potassium carbonate (mL)	2.7	1.0

Reducing solution was incubated for 50 min at 60°C in water bath and then quickly added to the $HAuCl_4$ containing 250 mL flask under intense stirring while keeping stir plate set to 60°C. Stirred solution was kept at this temperature for 30 min, followed by 10 min at 90°C, then cooled to r.t while stirring with heat turned off for 1 hour. 1 mL of 80mg/mL Bis(p-sulfonatophenyl) was then added and solution stirred overnight at r.t to improve particle stability. The size of all particles was confirmed by dynamic light scattering and transmission electron microscopy. The extinction coefficient for gold was calculated using plasmon absorption at 520 nm and the formula from (12). There was a small error in the published version; the corrected formula is as follows:

Extinction coefficient = $10^{(1.0643*LOG[3/2*3.141592654*(diameter)^3]+4.0935)}$

Synthesis of DNA and PEG functionalized GNPs. pH assisted method described previously was used (13). 15nm GNPs were concentrated in 1.5 mL Eppendorf tubes to 63nM in 0.01% (v/v) Tween-20 using 12,000g centrifugation for 35min. Concentration was quantified by measuring plasmon absorbance peak at 520 nm. For particles functionalized with ssDNA, 100μL of 63nM GNPs were mixed with 40μL of 0.1% (v/v) Twen-20, 60μL of ultrapure water, 100μL of 15μM of appropriate thiolated DNA and incubated for 5 min at r.t. 100μL of 100mM trisodium citrate pH 3 buffer was then added to neutralize negative charge of DNA backbone, and solution incubated at r.t. for 30 min allowing thiols on DNA strands to form bonds with gold nanoparticle surface. Gold surface was not efficient at reducing the 6-member diThiol containing ring of DNA25-(*diThiol*) and DNA45-*5'(diThiol)* strands, so this nucleotide was reduced with tris(2-carboxyethyl)phosphine (TCEP; 90μL of 100μM diThiol DNA incubated with 10μL of 100mM TCEP for 1hr at r.t.), purified by NAP-5 column

(GE Healthcare, Little Chalfont, UK), its concentration determined by measuring OD at 260 nm and adjusted to 15μM before adding it to nanoparticles. For the nanoparticles requiring PEG backfill, 50μL of 2mM of appropriate molecular weight mPEG-SH (terminated with methoxy on one end and a thiol on the other end) was added, and mixture incubated at 60°C for 30 min. Nanoparticles were then washed by 3 rounds of centrifugation (16,000g, 45 min each) in PBS supplemented with 0.01% (v/v) Tween-20 (PBST), and final concentration adjusted to 225nM.

For the experiments involving dsDNA, 150μL of 63nM GNPs were mixed with 40μL of 0.1% (v/v) Twen-20, 60μL of ultrapure water, 100μL of 15μM of appropriate thiolated DNA and incubated for 5 min at r.t. 150μL of 100mM trisodium citrate pH 3 buffer was then added and solution incubated at r.t. for 30 min. Nanoparticles were then washed by 2X centrifugation (16,000g, 35 min each) in PBST and their concentration adjusted to 25nM. 325μL of 25nm GNPs were then mixed with 130μL of appropriate 15μM cDNA for dsDNA particles, or 130μL of water for ssDNA particles. To this 375μL of 10X PBS, 125μL of 50mM $MgCl_2$, 125μL of 0.1% (v/v) Tween-20, and 170μL of ultrapure water were added, and the solution incubated at 60°C for 10min, followed by 1hr incubation at 37°C to facilitate cDNA hybridization. 65μL of appropriate weight 2mM mPEG-SH was then added and solution further incubated for 1hr at 37°C. Nanoparticles were finally washed by 3X centrifugation (16,000g, 45 min each) and concentration adjusted to 225nM in PBST.

5nm and 3nm nanoparticles DNA adsorption was performed similarly, but using higher centrifugation speeds for particle concentration and washing (150,000g, 25min for 5nm and 250,000g, 35min for 3nm), and different reagent amounts (1.4mL of 500nM GNPs, 280μL of 0.1% (v/v) Tween-20, 234μL ultrapure water, 186μL of 15μM appropriate DNA, and 700μL of 100mM trisodium citrate pH3 buffer). 5nm and 3nm GNPs were not backfilled with PEG.

Quantification of DNA and PEG loading. Both nucleic acid and PEG loading were quantified by depletion. Following the incubation to adsorb these molecules onto nanoparticle surface (described in previous section), nanoparticles were pelleted by centrifugation (21,000g, 35min), and excess DNA and PEG molecules remaining in the supernatant collected. Concentration of nucleotides was quantified using the Quant-iT OliGreen ssDNA Detection Kit (Invitrogen). A standard curve was created by serial dilutions of known concentration of the DNA strand being quantified. Working solution of OliGreen was prepared by mixing 5μL of 200X OliGreen reagent concentrate with 50μL of 20X TE buffer (100mM Tris-HCl, 10mM EDTA, pH 7.5) and 945μL ultrapure water. 50μL of working solution was then mixed with 50μL of each sample in black 96-well plate and incubated for 10min in the dark at r.t. Sample fluorescence was then measured with fluorescence plate reader with 480nm excitation and 520nm emission.

PEG concentration was quantified using standard Ellman's assay for measuring thiols in solution. Standard curve was generated by serial dilutions of known concentration of PEG with the same molecular mass. Working solution was prepared by mixing 60μL of Ellman's reagent with 3mL of ultrapure water. 100μL of working solution was mixed with 50μL of each samples in clear 96-well plates and incubated for 15min at r.t. Plate reader was then used to measure absorbance at 412nm. In parallel, absorbance of the unprocessed sample was quantified at 260nm to quantify concentration of DNA. Contribution of thiols corresponding to the DNA was then subtracted from the total thiol concentration, yielding amount of PEG-specific thiols.

Visualization and quantification of serum-induced aggregate formation. Aggregate formation at the end of serum incubation could be measured by absorbance spectrum scan from 450nm to 900nm wavelength using UV-Vis Spectrometer. More quantitative results for serum-induced aggregation were obtained by collection of the aggregate pellet (500g centrifugation, 5min), re-dispersing nanoparticles by 60min 37°C incubation with 310μL of PBST, 3.9μL of 20mg/mL Proteinase K, and (when indicated) 47μL of 5% SDS. Nanoparticle concentration was quantified by absorbance measurement at 520 nm.

Synthesis of single-layer assembled structures. In the first step 15nm GNPs functionalized with *Core-1* DNA were hybridized to *Linker-1* DNA at grafting ratio of 100 strands per nanoparticle (see Suppl. Fig. S18 for molecular details). 200μL of 25nM 15nm GNPs functionalized with *Core-1* DNA were mixed with 64uL of 8μM *Linker-1*, 216μL of 10X PBS, 70μL of 50mM $MgCl_2$, 70μL of 0.1% (v/v) Tween-20, and 80μL ultrapure water. In the case of 'Reduced Satellites' structures, 4μM *Linker-1* was used instead to reduce Linker to core GNP grafting ratio to 50. The mixture was incubated for 10min at 60°C, then for 60min at 37°C, purified by 2X centrifugation (16,000g, 35 min each) in PBST, and concentrated to 40nM. In the second step, the satellites were hybridized to the opposite end of *Linker-1* DNA with loading ratios of 160 satellites per core

nanoparticle. 50uL of 25nM Linker-hybridized 15nm GNPs were mixed with 400μL of 500nM 5nm GNP satellites functionalized with *Sat-1* strand, 300μL of 10X PBS, 100μL of 50mM $MgCl_2$, 100μL of 0.1% (v/v) Tween-20, and 50μL of ultrapure water, and solution incubate for 60min at 37°C. 150μL of 2mM 10 kDa mPEG-SH was then added as backfill (2400 PEG per satellite nanoparticle) and structures incubated for another 60min at 37°C, then purified by 3X centrifugation (11,000g, 35min each) and re-suspended in 25μL of PBST (final concentration ~50 nM). In the case of 'Short Linker' structures, *Core-2*, *Linker-2* and *Sat-2* strands were used instead.

Synthesis of 2-layer assembled structures. *Linker-1* strand was hybridized to *Core-1* functionalized nanoparticles as described for single-layer assemblies. In the next step a second internal layer of satellites was hybridized before loading of the outer layer satellites. 50uL of 25nM Linker-hybridized 15nm GNPs were mixed with 400μL of 500nM 5nm GNP satellites functionalized with *Sat-3* strand, 300μL of 10X PBS, 100μL of 50mM $MgCl_2$, 100μL of 0.1% (v/v) Tween-20, and 50μL of ultrapure water. The solution was incubated for 60min at 37°C, then further mixed with 400μL of 500nM 5nm GNP satellites functionalized with *Sat-1* DNA, 300μL of 10X PBS, 100μL of 50mM $MgCl_2$, 100μL of 0.1% (v/v) Tween-20, and 50μL of ultrapure water. The solution was incubated for 30min at 37°C to hybridize the outer satellite layer. 300μL of 2mM 5 kDa or 10 kDa mPEG-SH was then added as backfill (2400 PEG per satellite nanoparticle) and structures incubated for another 60min at 37°C then purified by 3X centrifugation (8,000g, 45min each) and re-suspended in 25μL of PBST (final concentration ~50 nM). Cargo loaded structures were generated in a similar manner, but *FAM* labeled *Sat-1* and *Cy5* labeled *Sat-3* strands were used.

Serum incubation of DNA-functionalized GNPs

4μL of 350nM GNP-DNA were added to 96μL of undiluted mouse serum (96μL PBS used as untreated control). *Serum incubation with actin:* 4μL of 350nM GNP-DNA, 91μL Serum, 5μL of 1mg/mL actin (or 5μL of 1X PBS as control). *DNase I incubation:* 4μL of 350nM GNP-DNA, 5μL of 1U/μL DNase I, 10μL of 10X DNase I reaction buffer (100mM Tris-HCl, 25mM $MgCl_2$, 1mM $CaCl_2$, pH 7.5), 71μL of PBS, 10μL of 1mg/mL actin (or 10μL ultrapure water as control). *Incubation with serum fractions*: 96μL of each serum fraction was used instead of serum. 'Protein' and 'small molecule' fractions were generated by passing 500μL of undiluted or 10X diluted (in PBS) serum through 10kDa Amicon Ultra 0.5 mL centrifugation filter. The pass-through fraction containing small molecules was used directly. The filtrate protein fraction was adjusted back to 500μL using PBS supplemented with calcium and magnesium. *Incubation with DTT:* 4μL of 350nM GNP-DNA, 10μL of 10X PBS, 10μL of 100mM DTT, 76μL of ultrapure water. *Incubation with GSH/Cysteine:* 4μL of 350nM GNP-DNA, 10μL of 10X PBS, 10μL of 200μM L-Cysteine, 10μL of 210μM GSH, 66μL of ultrapure water. *Serum incubation of free DNA:* 4μL of 100μM of stock DNA were added to 96μL of undiluted mouse serum. In each case multiple tubes were set up and each incubated for 0.5, 1, 2, 4, 6, or 8 hours at 37°C. *PAGE Gel visualization and quantification of degradation:* At the end of incubation, 3.9μL of 20mg/mL Proteinase K, 47μL of 5% SDS, and 310μL of PBST were added and solution incubated for 60min at 37°C to inactivate the proteins. Nanoparticles were washed by 2X centrifugation (16,000g, 35min each), and re-suspended in 100μL of TBE (89mM Tris, 89mM boric acid, 2mM EDTA, pH 8.3) supplemented with 0.01% Tween-20 (*TBET*). 10μL of 1M DTT was added to each tube and solution incubated at 60°C for 35min to release any remaining DNA strands into solution. The samples were centrifuged at 21,000g for 35 min and 60μL of supernatant collected. 10μl of each sample were mixed with 2μl of gel loading dye, and 10μl of this mixture loaded into 20% TBE PAGE gel. 10μL of ladder mixture (1ul single-stranded molecular standard (IDT), 9ul TBET, 2μL gel loading dye) was included in one of the wells. The gel was run for 70min at 200V, stained for 30min at r.t. with 7mL of 10X Sybr GOLD solution, and band migration visualized with Kodak fluorescence *in vivo* imager. Obtained image was processed with Image J software (background subtraction, noise removal, contrast and saturation adjustment).

Serum incubation of assembled structures

4μL of ~80nM of assembled structures was added to 96μL of undiluted mouse serum in multiple tubes and each tube incubated for 2, 4, 6, or 8 hours (and 12 and 16 hours for the 2-layer assemblies) at 37°C. *TEM visualization and quantification of degradation:* After incubation the particles were washed by 2X centrifugation (12,000g, 35 min each) and re-suspended in 10μL of PBS. 3μL of this solution was loaded onto a plasma treated TEM grid and imaged by FEI Tecnai 20 electron microscope (Advanced Bioimaging Centre, Mount Sinai Hospital, Toronto, Canada). *Tracking degradation and cargo release from 2-layer structures:* At the end of serum incubation particles were washed by 2X centrifugation (12,000g, 35min each) and re-

suspended in 100μL of PBS. 10μL were used for TEM measurements. 10μL of 1M DTT were added to remaining 90μL and mixture incubated for 30min at 60°C to release all remaining DNA conjugated dyes into solution. Nanoparticles were removed by centrifugation (21,000g, 30 min) and 60μL of supernatant collected. Amount of dye in solution was measured by Shimadzu UV-Visible spectrophotometer UV-1601PC. FAM was excited at 488nm and peak emission measured at 512nm. Cy5 was excited at 640nm and emission measured at 670nm. Degradation rates for TEM and fluorescent measurements were obtained by fitting the data with a single-phase decay curve.

REFERENCES

1. Storhoff JJ, et al. (2000) What Controls the Optical Properties of DNA-Linked Gold Nanoparticle Assemblies? *J Am Chem Soc* 122(19):4640–4650.

2. Betzel C, et al. (1993) Structure of the complex of proteinase K with a substrate analogue hexapeptide inhibitor at 2.2-A resolution. *J Biol Chem* 268(21):15854–15858.

3. Chinen AB, Guan CM, Mirkin CA (2015) Spherical Nucleic Acid Nanoparticle Conjugates Enhance G-Quadruplex Formation and Increase Serum Protein Interactions. *Angew Chem Int Ed* 54(2):527–531.

4. Albanese A, et al. (2014) Secreted Biomolecules Alter the Biological Identity and Cellular Interactions of Nanoparticles. *ACS Nano* 8(6):5515–5526.

5. Perrault SD, Walkey C, Jennings T, Fischer HC, Chan WCW (2009) Mediating Tumor Targeting Efficiency of Nanoparticles Through Design. *Nano Lett* 9(5):1909–1915.

6. Walkey CD, Olsen JB, Guo H, Emili A, Chan WCW (2012) Nanoparticle size and surface chemistry determine serum protein adsorption and macrophage uptake. *J Am Chem Soc* 134(4):2139–2147.

7. Dai Q, Walkey C, Chan WCW (2014) Polyethylene Glycol Backfilling Mitigates the Negative Impact of the Protein Corona on Nanoparticle Cell Targeting. *Angew Chem Int Ed* 53(20):5093–5096.

8. Larson TA, Joshi PP, Sokolov K (2012) Preventing Protein Adsorption and Macrophage Uptake of Gold Nanoparticles viaa Hydrophobic Shield. *ACS Nano* 6(10):9182–9190.

9. Song L, et al. (2015) Terminal PEGylated DNA-Gold Nanoparticle Conjugates Offering High Resistance to Nuclease Degradation and Efficient Intracellular Delivery of DNA Binding Agents. *ACS Applied Materials Interfaces* 7(33):18707–18716.

10. Gref R, et al. (2012) The controlled intravenous delivery of drugs using PEG-coated sterically stabilized nanospheres. *Adv Drug Deliv Rev* 16:215–233.

11. Iciek M, Chwatko G, Lorenc-Koci E, Bald E, Wlodek L (2004) Plasma levels of total, free and protein bound thiols as well as sulfane sulfur in different age groups of rats. *Acta Biochim Pol* 51(3):815–824.

12. Perrault SD, Chan WCW (2009) Synthesis and Surface Modification of Highly Monodispersed, Spherical Gold Nanoparticles of 50–200 nm. *J Am Chem Soc* 131(47):17042–17043.

13. Zhang X, Servos MR, Liu J (2012) Instantaneous and Quantitative Functionalization of Gold Nanoparticles with Thiolated DNA Using a pH-Assisted and Surfactant-Free Route. *J Am Chem Soc* 134(17):7266–7269.